RESEARCH ARTICLE

Key Points:
- Changes in GIM-TEC of the ionosphere are compared with occurrences of $M \geq 6.0$ earthquakes globally for 2000-2014
- No statistically significant changes in GIM-TEC prior to earthquakes
- No evidence that monitoring changes in GIM-TEC might be useful for predicting earthquake occurrence

A statistical study of global ionospheric map total electron content changes prior to occurrences of $M \geq 6.0$ earthquakes during 2000–2014

J. N. Thomas[1,2,3] (iD)**, J. Huard[1,2,4], and F. Masci[5]** (iD)

[1]NorthWest Research Associates, Redmond, Washington, USA, [2]Department of Electrical and Computer Engineering, DigiPen Institute of Technology, Redmond, Washington, USA, [3]Department of Earth and Space Sciences, University of Washington, Seattle, Washington, USA, [4]Department of Aerospace Engineering Sciences, University of Colorado Boulder, Boulder, Colorado, USA, [5]Istituto Nazionale di Geofisica e Vulcanologia, L'Aquila, Italy

Abstract There are many reports on the occurrence of anomalous changes in the ionosphere prior to large earthquakes. However, whether or not these changes are reliable precursors that could be useful for earthquake prediction is controversial within the scientific community. To test a possible statistical relationship between ionospheric disturbances and earthquakes, we compare changes in the total electron content (TEC) of the ionosphere with occurrences of $M \geq 6.0$ earthquakes globally for 2000–2014. We use TEC data from the global ionosphere map (GIM) and an earthquake list declustered for aftershocks. For each earthquake, we look for anomalous changes in GIM-TEC within 2.5° latitude and 5.0° longitude of the earthquake location (the spatial resolution of GIM-TEC). Our analysis has not found any statistically significant changes in GIM-TEC prior to earthquakes. Thus, we have found no evidence that would suggest that monitoring changes in GIM-TEC might be useful for predicting earthquakes.

1. Introduction

Despite several published studies [see. e.g., *Heki and Enomoto*, 2013, 2015; *Le et al.*, 2011; *Li and Parrot*, 2013], the occurrence of earthquake precursory signals in the ionosphere is controversial within the scientific community, and validated physical generation mechanisms of possible precursory ionospheric anomalies are not yet identified. Local conditions of the ionosphere are subject to numerous influences such as solar activity, geomagnetic activity, meteorological events, anthropogenic effects, atmospheric gravity waves, and traveling ionospheric disturbances. The ionosphere also shows normal seasonal, day-to-day, and diurnal variations. Thus, it is difficult to clearly identify preseismic ionospheric changes that may be considered as possible precursors. For instance, one published report [*Le et al.*, 2011] using a statistical analysis of global ionosphere map-total electron content (GIM-TEC) data claims to have found such a signal, an increase in GIM-TEC anomalies in the days leading up to earthquakes. *Le et al.* [2011] studied 736 $M \geq 6.0$ earthquakes globally during 2002–2010 and found that the occurrence rates of what they called abnormal GIM-TEC days are increased for earthquakes with depths less than 20 km and magnitudes greater than about M6.7. Other studies, however, have found no relationship between preearthquake TEC changes and earthquakes [see, e.g., *Afraimovich and Astafyeva*, 2008; *Astafyeva and Heki*, 2011; *Dautermann et al.*, 2007]. *Dautermann et al.* [2007] found no statistically significant correlation between preearthquake TEC anomalies and the earthquake occurrences in Southern California for the 2003–2004 period. More recently, some reviews [see *Masci*, 2012, 2013; *Masci and Thomas*, 2014; *Masci et al.*, 2015; *Thomas et al.*, 2012] have demonstrated that reported preearthquake ionospheric changes are not uniquely associated with seismic activity. These authors do not disprove the possible existence of precursory phenomena, but they have shown that even during periods of low solar and geomagnetic activity [see also *Astafyeva and Heki*, 2011], changes in preearthquake TEC are driven by changes in solar and geomagnetic activities which may induce not only global changes in the ionosphere but also changes in ionospheric parameters, such as TEC, on regional scales [see also *Afraimovich and Astafyeva*, 2008].

In this paper, we conduct a straightforward analysis of preseismic and coseismic changes in GIM-TEC for all global $M \geq 6.0$ earthquakes during 2000–2014 in order to test a possible statistical significance between TEC changes and seismic activity. Since the GIM-TEC data have a time resolution of 2 h, our study focuses on ionospheric changes that occur several days before earthquakes and with a duration of many hours to
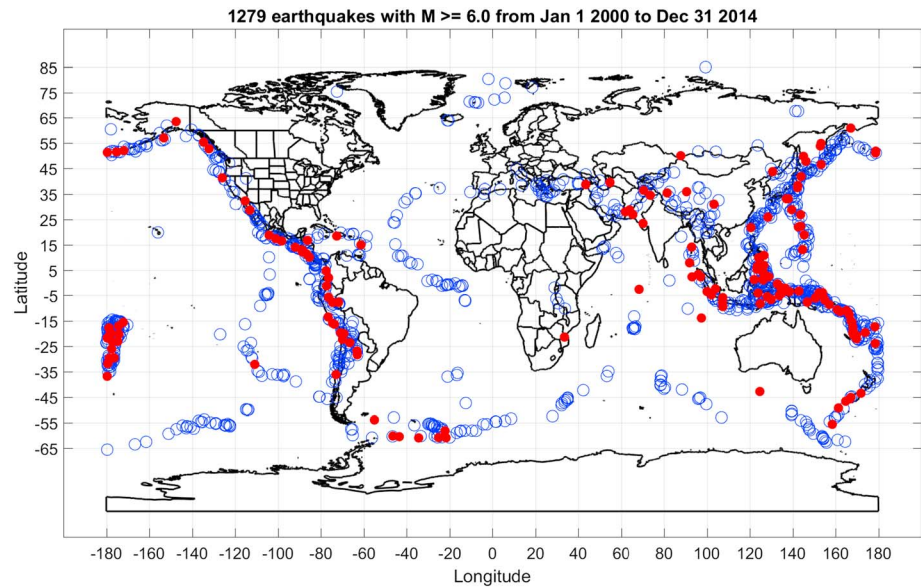
Figure 1. Map of earthquake data set $M \geq 6.0$ during 2000–2014. The red dots are earthquakes with $M \geq 7.0$.

days. Short-duration TEC changes that have been reported to occur several tens of minutes before earthquakes and with a duration of less than 1 h are not investigated because these changes cannot be resolved by GIM-TEC data. However, among the reported short-duration TEC changes are 40 min preearthquake TEC changes identified by *Heki and Enomoto* [2013] whose reliability as precursors have been recently questioned [see, e.g., *Kamogawa and Kakinami*, 2013; *Masci et al.*, 2015].

2. Data Sets and Methods

The data sets used in this study include earthquake data and GIM-TEC ionosphere data. A list of 1279 $M \geq 6.0$ earthquakes for 2000–2014 globally and declustered for aftershocks was provided by Andrew Michael from the USGS (United States Geological Survey) [*Michael*, 2011]. Figure 1 shows the locations of these earthquakes, and Table 1 shows their distribution by magnitude and depth. Ionospheric data used are TEC maps derived from GPS signals. The phases of GPS satellite signals (1575.42 and 1227.60 MHz carrier frequencies), transmitted to ground stations through the ionosphere, are affected by the path-integrated electron density known as slant TEC (STEC, measured in TEC units, where 1 TECU = 10^{16} el/m^2). By monitoring the phase difference of the two GPS signals, we can get the temporal changes of STEC. We examine the vertical TEC (VTEC), which is the integrated electron density in the vertical column of the ionosphere above each station [*Komjathy et al.*, 2005]. Using VTEC from 200+ GPS receivers worldwide, NASA's Jet Propulsion Laboratory (JPL) produces global ionosphere maps of TEC with a cadence of 2 h. GIM-TEC covers ±87.5° of latitude and ±180° of longitude with a spatial resolution of 2.5° and 5.0°, respectively. We obtained GIM data from JPL for 2000–2014 (ftp://cddis.gsfc.nasa.gov/pub/gps/products/ionex). The GIM-TEC data are a superset of the data used by *Le et al.* [2011] for their study of 2002–2010 earthquakes.

Our statistical analysis procedure for comparing earthquake occurrences with GIM-TEC data is as follows. As in *Le et al.* [2011], we find the GIM-TEC data point closest to earthquake location and use linear interpolation to get a GIM-TEC value each hour. Then, still following their method, we remove geomagnetically disturbed days which are identified by $Dst < -40$ nT (where Dst is the geomagnetic disturbance storm time index) or by the decrease in amplitude of Dst index within a day larger than 40 nT. We also remove GIM-TEC time series data within ±1 day of any GIM-TEC data dropout. We then apply a 24 h running average filter to the GIM-TEC data (at that location and for ±30 days of the earthquake day) to remove diurnal variations. We also detrend the GIM-TEC data by finding the cubic fit residual to remove seasonal effects. We calculate the mean μ and the standard deviation σ of filtered and detrended GIM-TEC time series for ±30 days of earthquakes. Then, we count the number of hourly GIM-TEC values that exceed ±2σ per day for ±15 days of earthquakes. Similar to *Le et al.* [2011] that looked for possible precursors within 15 days prior to earthquakes, we use

Table 1. Distribution by Magnitude and Depth of the Earthquakes During 2000–2014

Magnitude	Depth (km)			
	<20	<30	<40	Inf
6	134	149	183	254
6.1	102	122	143	194
6.2	66	76	92	138
6.3	76	85	101	141
6.4	49	58	72	101
6.5	39	49	57	85
6.6	44	49	52	75
6.7	27	33	37	49
6.8	18	21	25	43
6.9	16	23	23	35
7	10	15	19	26
7.1	6	6	10	22
7.2	5	7	9	16
7.3	6	8	11	19
7.4	4	6	6	11
7.5	2	4	8	12
7.6	5	10	12	16
7.7	5	5	6	12
7.8	3	4	7	9
7.9	3	3	4	5
8	0	1	3	4
8.1	2	3	3	3
8.2	0	1	1	1
8.3	1	2	2	3
8.4	0	0	1	1
8.5	0	0	0	0
8.6	1	1	1	1
8.7	0	0	0	0
8.8	0	1	1	1
8.9	0	0	0	0
9	0	2	2	2
	624	744	891	1279

±15 days to count values that exceed $\pm2\sigma$. We combine results for all earthquakes binned by magnitude and depth, and we calculate the percentage of earthquakes that are associated with GIM-TEC values that exceed $\pm2\sigma$ per day binned by magnitude and depth. In the supporting information, we also show GIM-TEC deviations that exceed $\pm1\sigma$ and $\pm3\sigma$ for ±15 days of earthquakes and the results of the GIM-TEC analysis in which we use $Kp > 3$ (where Kp is the planetary geomagnetic index) to remove GIM-TEC data related to geomagnetically disturbed days. Lastly, the supporting information includes results by using a 24 h notch filter rather than a 24 h running average.

3. Case Studies

We start by looking at example case studies for two large earthquakes. Figures 2 and 3 show case studies of ±30 days of raw and 24 h filtered/detrended GIM-TEC data for the 11 March 2011 Tohoku, Japan, *M*9.0 earthquake and the 27 February 2010 Chile *M*8.8 earthquake. Like described in section 2, we show GIM-TEC data points closest to the earthquake location. The time series in red show the *Dst* disturbed days (or time series within ±1 day of GIM-TEC data dropouts), and the time series in green are for the earthquake day. The horizontal dotted lines are the mean and 1, 2, and 3σ deviations. The raw time series in Figures 2a and 3a show a strong diurnal signal and a weaker longer-term (up to 30 days) trend. Changes that have a duration of a few days are also seen, which are often related to geomagnetic activity. In the 24 h filtered/detrended time series in Figures 2b and 3b, the diurnal variations and long-term trends are removed. In Figures 2 and 3 there are no clear preseismic changes in GIM-TEC data that can be associated with the earthquake. More precisely, in Figure 2b when we consider a time window of ±15 days, we can see an increase in GIM-TEC data during a few days before the Tohoku earthquake that might be interpreted as seismogenic. However, by
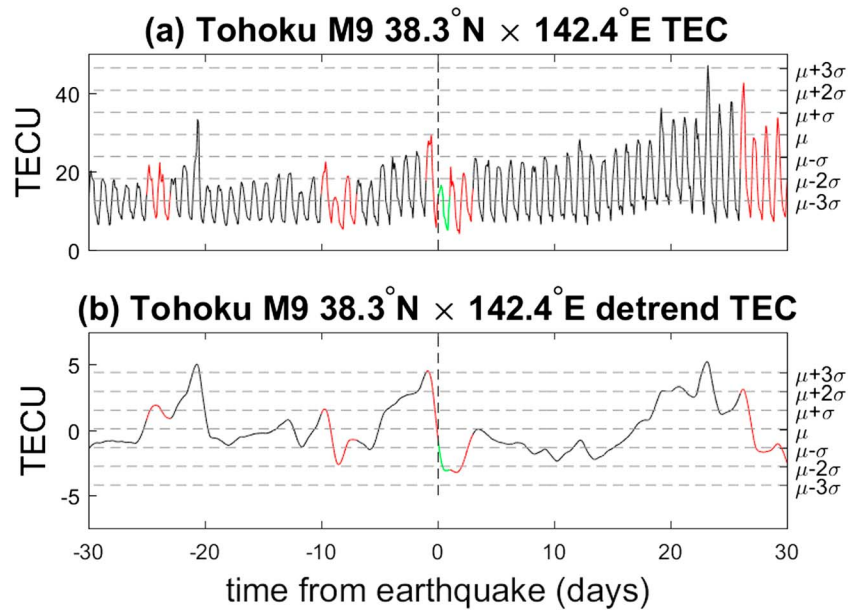
Figure 2. Case study 2 month TEC time series: (a) Raw and (b) 24 h filtered/detrended TEC time series for the 11 March 2011 Tohoku, Japan, earthquake. The time series in red shows the *Dst* disturbed days, and the time series in green is for the earthquake day. The horizontal dotted lines are the mean and 1, 2, and 3σ deviations. Negative days are before the earthquake occurrence.

considering a larger time windows of ±30 days we can see GIM-TEC increases having similar amplitude and time duration approximately 3 weeks before and 3 weeks after the earthquake day. Similarly, in Figure 3b we see an increase in GIM-TEC both about 2 weeks before and after the earthquake date.

To give a more panoramic view, Figures 4 and 5 show (a) raw, (b) 24 h filtered/detrended, and (c) 1 month filtered 15 year GIM-TEC time series for the Tohoku and Chile earthquakes. In this much longer time series,
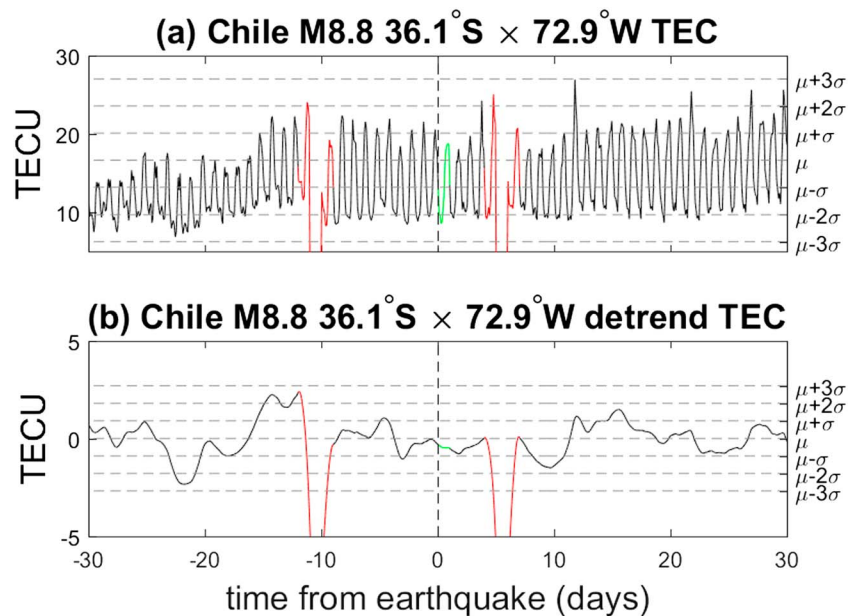

Figure 3. Case study 2 month TEC time series: (a) Raw and (b) 24 h filtered/detrended TEC time series for the 27 February 2010 Chile earthquake. The time series in red shows the *Dst* disturbed days, and the time series in green is for the earthquake day. The horizontal dotted lines are the mean and 1, 2, and 3σ deviations. Note that the large decreases near day −11 and day 6 are due to gaps in GIM-TEC data. Negative days are before the earthquake occurrence.
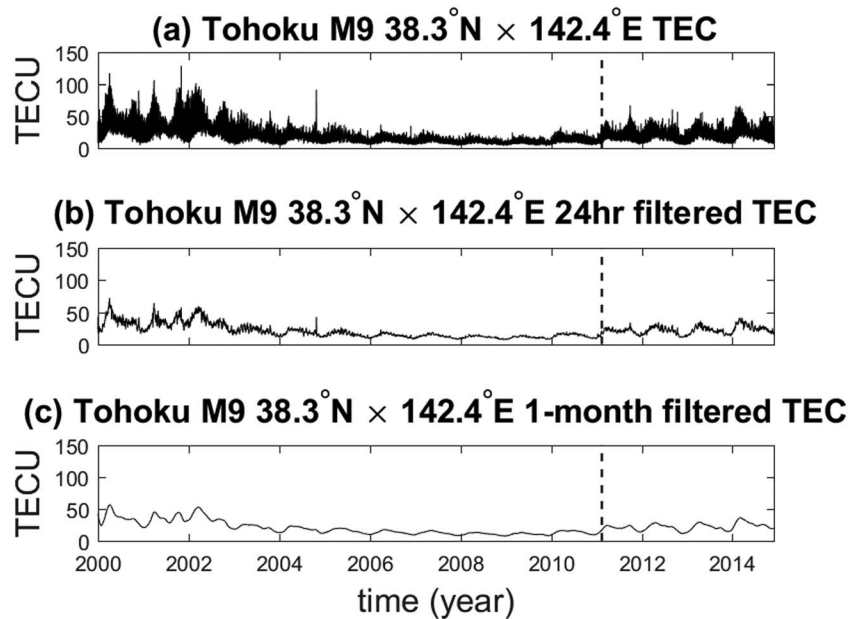
Figure 4. 15 year GIM-TEC time series: (a) Raw and (b) 24 h filtered/detrended, and (c) 1 month filtered GIM-TEC time series for the location of the 11 March 2011 Tohoku, Japan, earthquake.

the yearly and 11 year solar cycle variations are seen. Just as in Figures 2 and 3, here we do not see evidence of clear preseismic changes in GIM-TEC data.

4. Statistical Results

As we did for the case studies in section 3, we have processed GIM-TEC for the 1279 earthquakes in Figure 1 and Table 1 by using the methods described in section 2. Figure 6 shows the percentage of earthquakes that have GIM-TEC $\pm 2\sigma$ deviations organized by magnitude and depth. Here the percentage is defined as the ratio
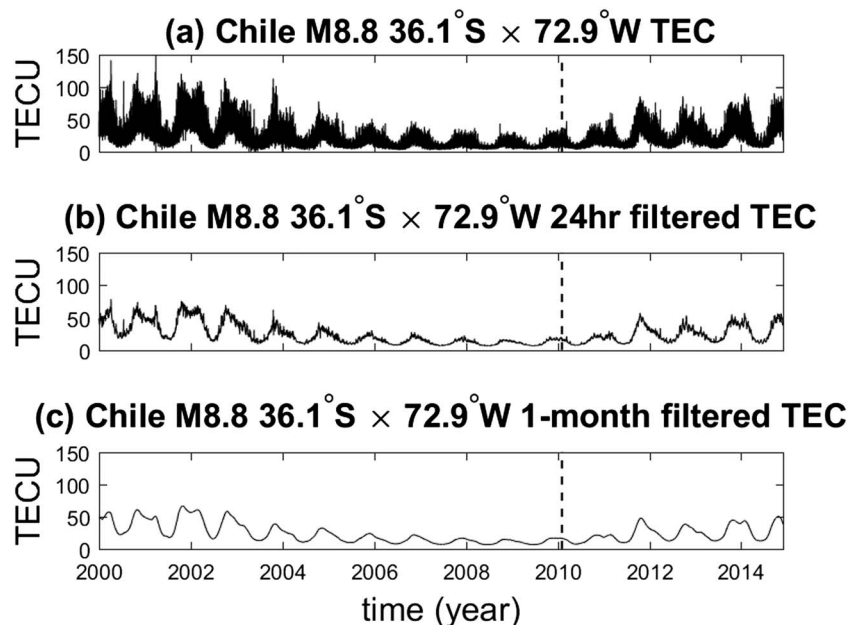

Figure 5. 15 year GIM-TEC time series: (a) Raw and (b) 24 h filtered/detrended, and (c) 1 month filtered GIM-TEC time series for the location of the 27 February 2010 Chile earthquake.
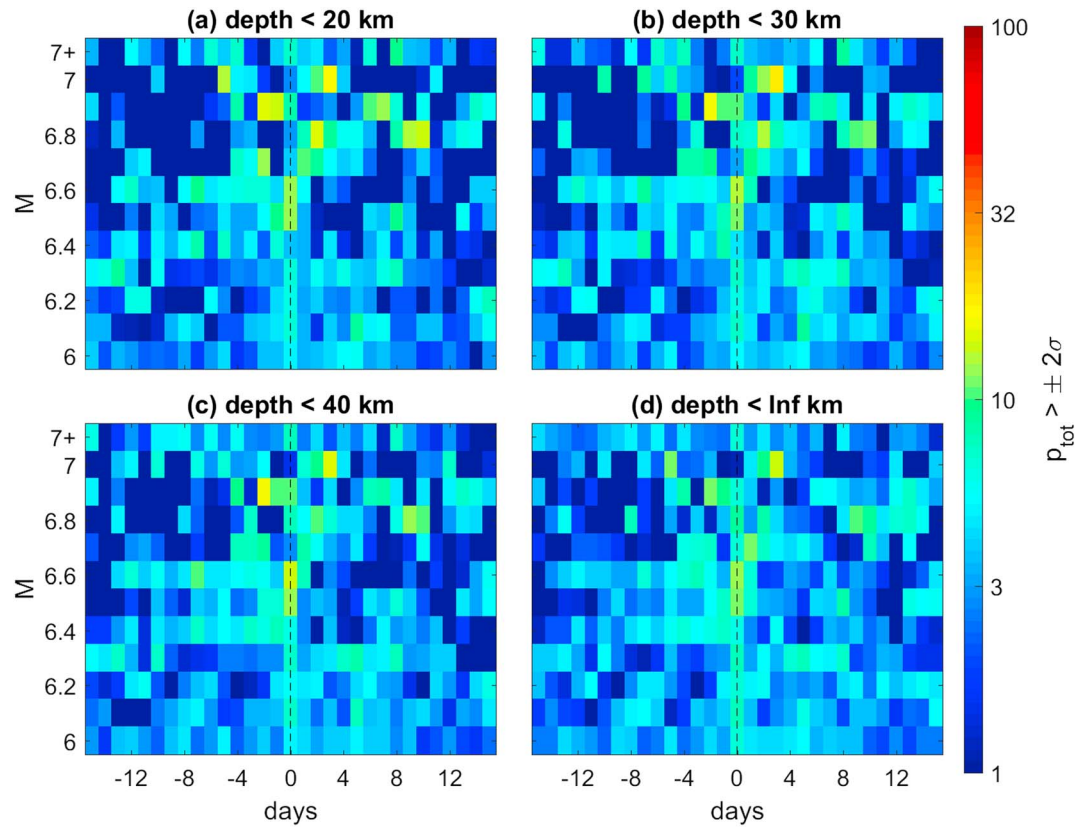
Figure 6. Statistical results per hourly data samples. Percentage of earthquakes that have GIM-TEC $> \pm 2\sigma$ deviations organized by magnitude and depth. Percentage (p_{tot}) is the ratio of the number of GIM-TEC hourly values exceeding $\pm 2\sigma$ to the total number of GIM-TEC hourly values. Negative days are before the earthquake occurrence.

of the number of GIM-TEC hourly values exceeding $\pm 2\sigma$ ($\text{TEC}_{2\sigma}$) to the total number of GIM-TEC hourly values (n_{tot}). The percentage is given by $p_{tot} = \frac{\text{TEC}_{2\sigma}}{n_{tot}} \times 100\%$. A weak increase (about 15%) in the percentage of $\pm 2\sigma$ changes can be seen on the earthquake day (day 0), which might be related to well-established coseismic effects [e.g., *Astafyeva et al.*, 2011; *Hao et al.*, 2012; *Occhipinti et al.*, 2013]. No significant increase in percentage is seen prior to earthquakes. Weak increases (up to 25%) can be seen for *M*6.9 earthquakes 2 to 3 days prior to the earthquake day and for *M*7.0 earthquakes 5 days (Figures 6a and 6d) prior to the earthquake day. However, similar increases can be sometimes seen in Figure 6 a few days after the earthquake as well. Note that results in Figure 6 do not take into account increasing error due to decreasing earthquake sample size, which occurs as earthquake magnitude increases.

Figure 7 show statistical results per day rather than per GIM-TEC samples shown in Figure 6. Here in Figure 7, percentage is the ratio of the number of earthquake days with at least one hourly GIM-TEC value exceeding $\pm 2\sigma$ ($\text{TEC}_{2\sigma\text{day}}$) to the total number of earthquake days (n_{day}). The percentage is given by $p_{day} = \frac{\text{TEC}_{2\sigma\text{day}}}{n_{day}} \times 100$ %. These percentages are higher than in Figure 6 because the percentage of days with at least one GIM-TEC value exceeding $\pm 2\sigma$ is greater than the percentage of total GIM-TEC values exceeding $\pm 2\sigma$. Weak increases (10–30%) are seen a few days before the earthquake day for *M*6.4 to *M*7.0 earthquakes. For *M*7.0 earthquakes, e.g., weak percentage increases are seen 2 to 6 days and 10 days before the earthquake day. However, also in Figure 7 similar increases can be seen a few days after the earthquake day.

To account for sample size error due to decreasing number of earthquakes with magnitude, in Figure 8 we have calculated the standard error of percentages in Figure 7. We use the standard error formula defined by $\text{stderr} = \sqrt{\frac{\frac{p_{day}}{100}\left(1 - \frac{p_{day}}{100}\right)}{n_{day}}} \times 100\%$. Here we see that the increased percentages found in Figure 7 at 2 to 6 days and 10 days before the earthquake day for *M*7.0 earthquakes have a larger error (10–25%).
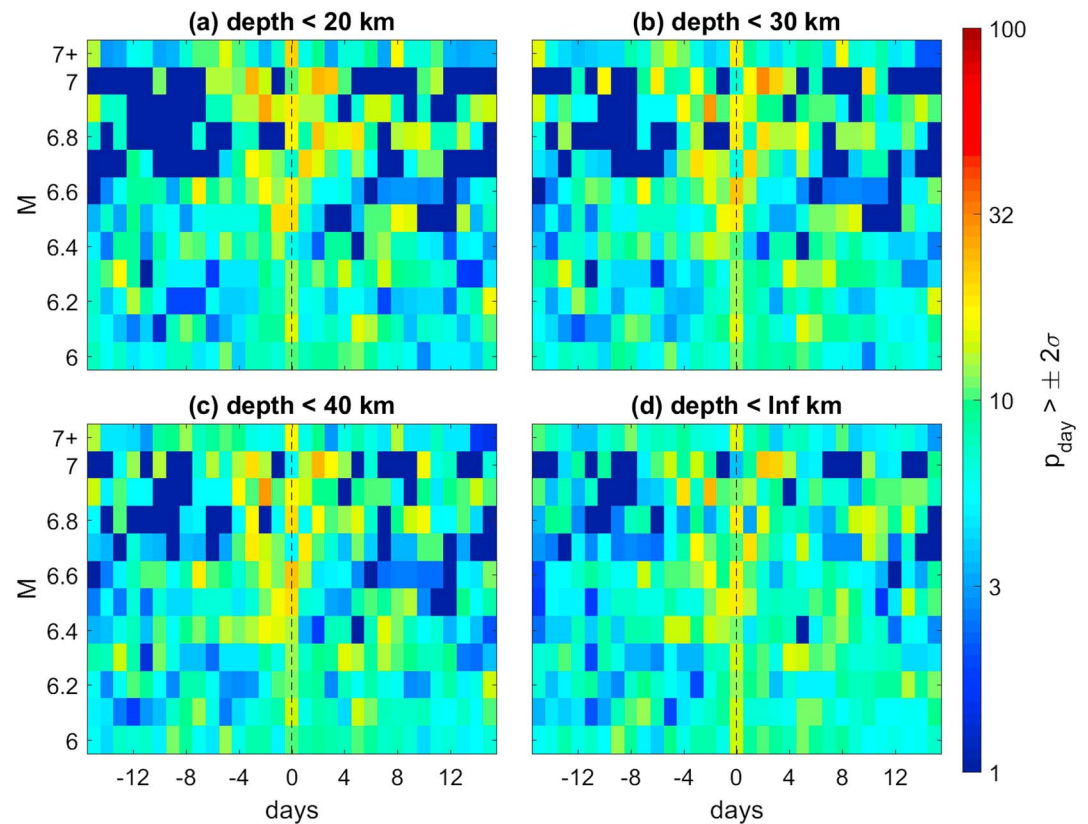
Figure 7. Statistical results per day. Percentage of earthquakes that have GIM-TEC $> \pm 2\sigma$ deviations organized by magnitude and depth. Percentage (p_{day}) is the ratio of the number of earthquake days with at least one-hourly GIM-TEC value exceeding $\pm 2\sigma$ to the total number of earthquake days. Negative days are before the earthquake occurrence.

To more clearly show how standard error due to earthquake sample size affects the statistical analysis, Figures 9 and 10 combine the percentages shown in Figure 7 and standard errors shown in Figure 8 for depth at <20 km and $M6.6$ through $M7.0+$. Of interest, Figure 10b shows percentages for depth at <20 km and $M7.0$ where a possible preseismic increase was observed in Figure 7. Here we see that although the percentages are not so high (about 15–30%), the standard errors (shown as error bars) are also large at about ± 10–15%. On the contrary, the low standard error shown in Figure 10a is due to the high sample size of the $M7+$ earthquakes (see Table 1). We thus conclude that the weak increase 2 to 6 days and 10 days before the earthquake day for $M7.0$ earthquakes is likely due to the low sample size of $M7$ earthquakes (10 earthquakes total for depth at <20 km according to Table 1).

We would like to point out that our results do not depend on using GIM-TEC values exceeding $\pm 2\sigma$. This is supported by our analyses shown in the supporting information where GIM-TEC deviations that exceed $\pm 1\sigma$ (Figures S1–S5 in the supporting information) and $\pm 3\sigma$ (Figures S6–S10) are used. Moreover, our results do not depend on using Dst criteria to remove geomagnetically disturbed days. In Figures S11–S25 we show the GIM-TEC analysis where $Kp > 3$ is used to remove disturbed days. Still, our results do not rely on the 24 h filter employed. In Figure S26, like in Figure 6, we show the p_{tot} analysis by using a 24 h notch filter rather than a 24 h running average.

5. Discussion and Conclusions

We find no evidence of significant changes in GIM-TEC prior to earthquakes in our statistical analysis of 1279 $M \geq 6.0$ earthquakes for 2000–2014. Our findings disagree with previous statistical studies of GIM-TEC and earthquakes [e.g., *Le et al.*, 2011]. *Le et al.* [2011] found (as shown in their Figure 4) that the occurrence rate of GIM-TEC anomalies increased, relative to background days, by a multiplicative factor of 2 to 3.5 during 1 to 5 days before earthquakes greater than $M6.4$ (especially greater than $M6.7$). In our analysis shown in
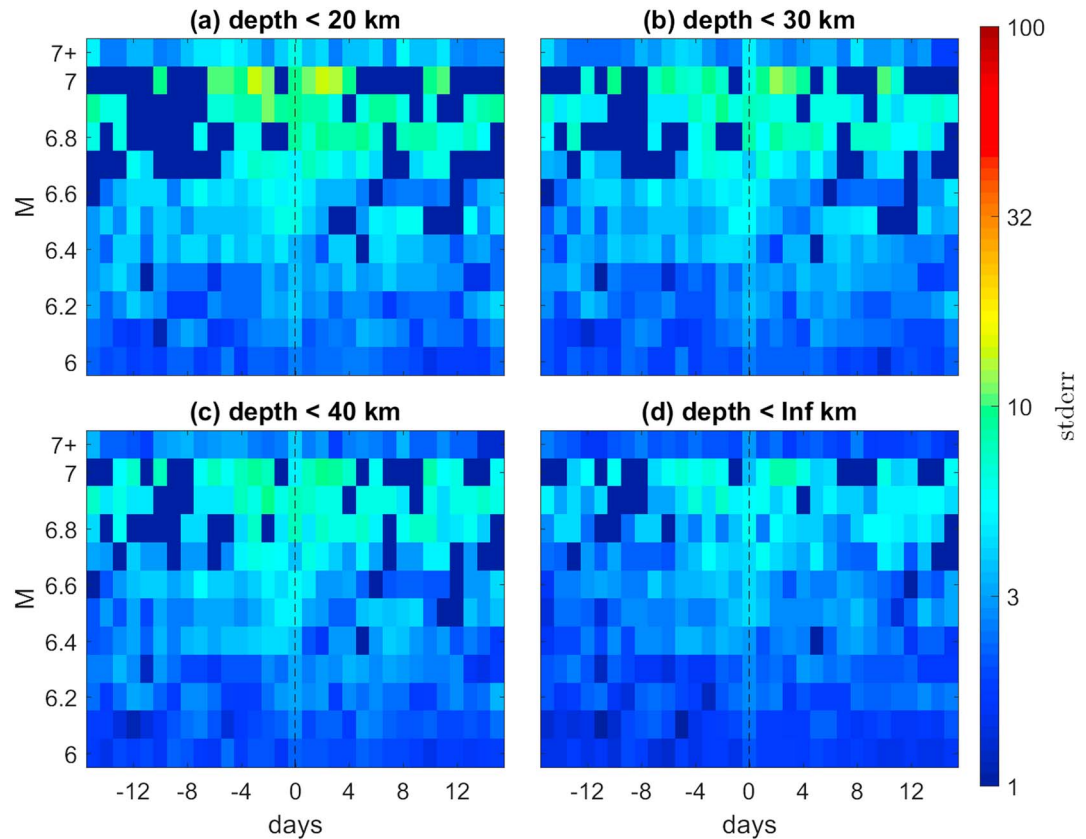
Figure 8. Standard error (stderr) for probabilities shown in Figure 7 to account for the decreasing number of earthquakes as magnitude increases.

Figure 7, we also see a weak increased percentage of GIM-TEC deviations a few days before the earthquake day for $M6.4$ to $M7.0$ earthquakes. However, for these earthquakes, and for earthquakes with other magnitudes, we see a similar increased percentage for a few days after the earthquake day as well. Unfortunately, we cannot compare these postseismic data with *Le et al.* [2011] because they do not present any data for days after the earthquake day. More importantly, we also find that the percentages in all cases (before and after the earthquake day) have errors that depend strongly on earthquake magnitude due to sample size effects. It is not clear how Le et al. accounted for sample size error in their quartile-based statistical analysis. Finally, we used a well-established list of earthquakes declustered for aftershocks [*Michael*, 2011]. Whereas *Le et al.* [2011, paragraph 5] declustered the aftershocks themselves by removing "earthquakes occurring at the similar location but with the short interval (<15 days) from the previous one."

We note that *Le et al.* [2011] calculated the occurrence of GIM-TEC anomalies within a certain day (for instance, 3 day mean anomalies occurring on days 1–3 are all included) and for earthquake magnitudes greater than or equal to a certain magnitude (for instance, 6.5 means all the earthquakes $\geq M6.5$). Whereas, in our analysis presented thus far, we calculate the occurrence of anomalies on a certain day and for a certain magnitude. To compare our results with those of Le et al., Figure 11 presents p_{day} results using the same accumulation method (within a certain day and greater than certain magnitude). Figure 11 shows that the accumulation method essentially applies a window filter and "smooths" the p_{day} statistics shown in Figure 7. Both Figures 7 and 11 show no evidence of significant GIM-TEC preearthquake changes, which means that our analysis is insensitive to the "on a certain day and for a certain magnitude" method.

An important point is whether the GIM-TEC data with a resolution of $2.5°$ latitude and $5.0°$ longitude and a cadence of 2 h can resolve possible preseismic or even coseismic TEC deviations. *Le et al.* [2011] argue that ionospheric earthquake precursors can affect an area large enough to be resolved by GIM-TEC data by citing the theoretical relationship reported by *Dobrovolsky et al.* [1979] between the size of the alleged preparation zone of an earthquake and its magnitude. However, the theoretical formula proposed by *Dobrovolsky et al.*
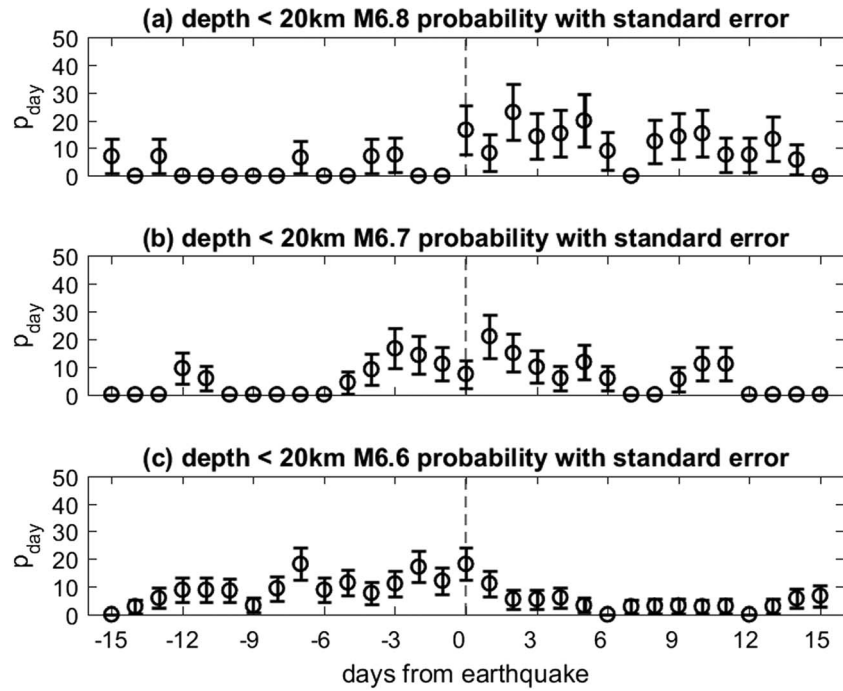
Figure 9. Percentages (p_{day}) shown in Figure 7 and standard errors shown in Figure 8 for depth at <20 km and (a) M6.8, (b) M6.7, and (c) M6.6.

[1979] is not supported by experimental evidence. Indeed, as pointed out by *Masci and Thomas* [2014], studies using GPS and satellite measurements have shown that the area involved in the preparation of an earthquake is much lower than that estimated by the theoretical calculation of Dobrovolsky. Consider that for a M9.0 earthquake, Dobrovolsky's formula estimates a preparation zone having a radius of more than 7000 km. This area is about one third of the Earth's surface. Thus, if we accept that precursory signals may
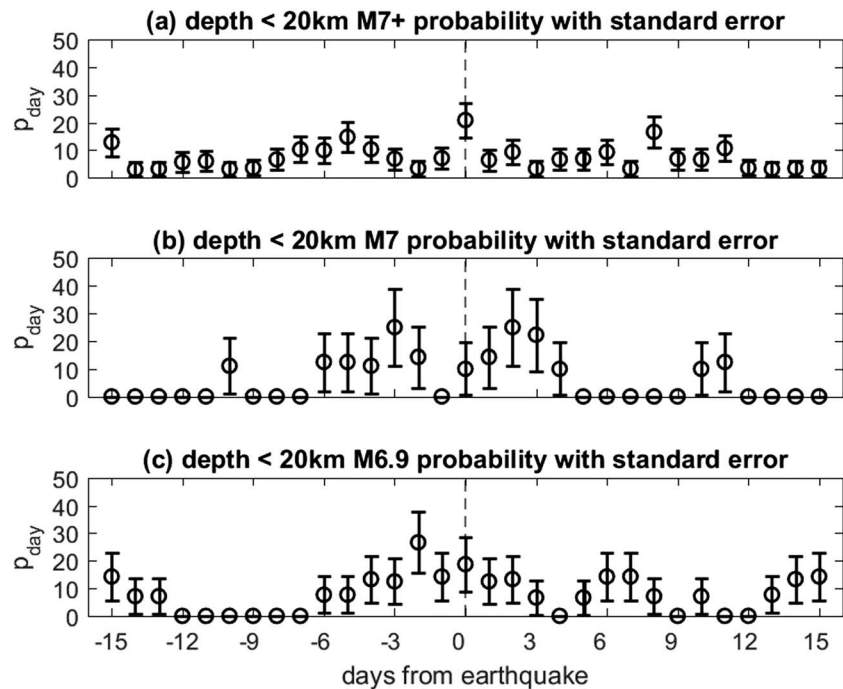

Figure 10. Percentages (p_{day}) shown in Figure 7 and standard errors shown in Figure 8 for depth at <20 km and (a) M7+, (b) M7.0, and (c) M6.9.
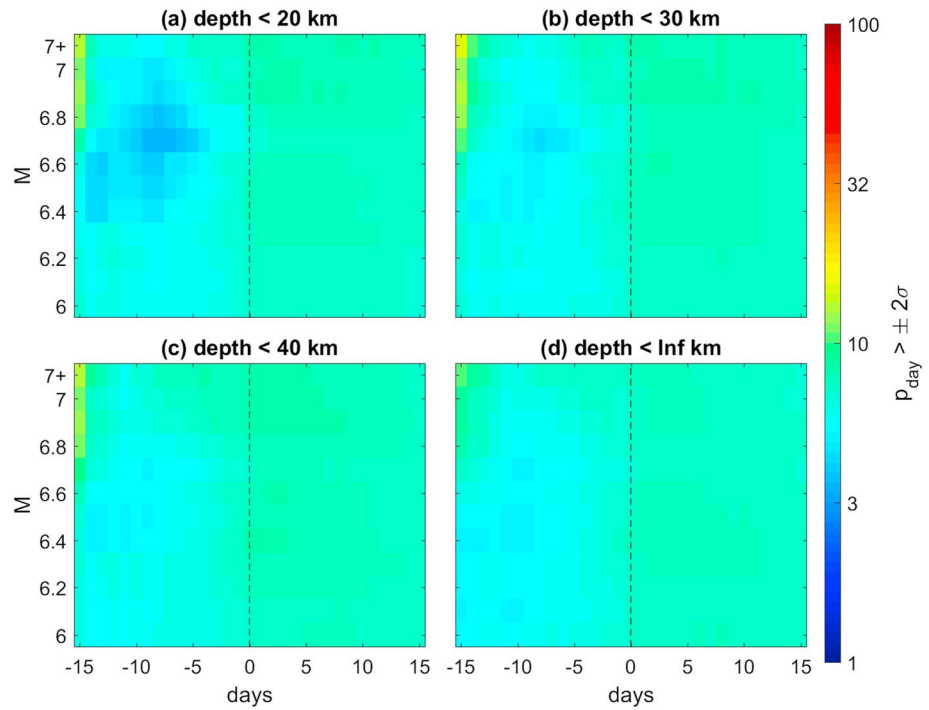
Figure 11. Statistical results per day (p_{day}), like those in Figure 7, but now calculating the occurrence of GIM-TEC anomalies within a certain day and for earthquake magnitudes greater than or equal to a certain magnitude (see text for details).

be observed in the area estimated by the Dobrovolsky's formula, then the alleged observed precursors are not useful for earthquake prediction.

Another point of interest is whether a ±15 day window is sufficient for searching for earthquake precursors. There have been some reports of possible precursors in ionospheric TEC or geomagnetic field data up to
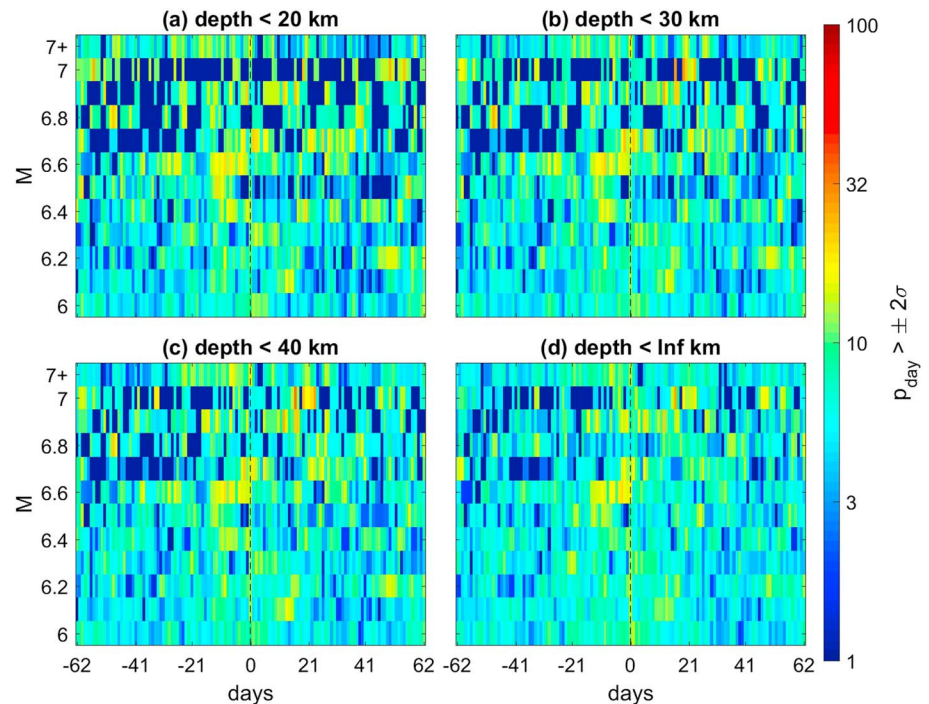

Figure 12. Statistical results per day (p_{day}), like those in Figure 7, but now using an extended window of ±2 months of earthquake occurrences.

2 months prior to earthquakes, such as *Xu et al.* [2013] for the 2011 Tohoku earthquake. Figure 12 shows GIM-TEC statistics (p_{day}) like in Figure 7, but now for an extended time window of ±2 months of earthquake occurrences. In agreement with our ±15 day analysis, in this broader time window we see no evidence of significant changes that might be considered as possible precursors.

In summary, our study does not provide clear evidence of statistically significant preseismic changes in GIM-TEC data that might occur several days before earthquakes and with duration of many hours to days. The percentage of earthquakes that show GIM-TEC preearthquake anomalies that exceed ±2σ are always less than about 25%, and the error increases with increasing earthquake magnitude. For example, results that show a possible increase in GIM-TEC anomalies for *M*7.0 earthquakes have a large error as shown in Figure 10. Moreover, our analysis does not provide any clear evidence of coseismic effects. The possible coseismic signals on the earthquake day in Figures 6 and 7 are really not particularly compelling, because the percentages are never greater than about 25% and not related to earthquake magnitude or depth. What this means is that any possible preseismic or even well-understood coseismic signals are not resolved by GIM-TEC data. This is not surprising because of the relatively poor resolution of GIM (2.5° latitude and 5.0° longitude and a cadence of 2 h), and possible earthquake effects in the ionosphere are expected to be somewhat localized and lasting a few hours [see, e.g., *Rolland et al.*, 2011]. Also, short-duration TEC changes that have been reported to occur several tens of minutes before earthquakes cannot be resolved by GIM-TEC data and are not addressed in our study. In conclusion, we find it very unlikely that GIM-TEC analysis can be used for identifying precursors or for earthquake prediction.

References

Afraimovich, E. L., and E. I. Astafyeva (2008), TEC anomalies-local TEC changes prior to earthquakes or TEC response to solar activity changes?, *Earth Planets Space*, 60, 961–966, doi:10.1186/BF03352851.

Astafyeva, E., and K. Heki (2011), Vertical TEC over seismically active region during low solar activity, *J. Atmos. Sol. Terr. Phys.*, 73(13), 1643–1652, doi:10.1016/j.jastp.2011.02.020.

Astafyeva, E., P. Lognonné, and L. Rolland (2011), First ionospheric images of the seismic fault slip on the example of the Tohoku-Oki earthquake, *Geophys. Res. Lett.*, 38, L22104, doi:10.1029/2011GL049623.

Dautermann, T., E. Calais, J. Haase, and J. Garrison (2007), Investigation of ionospheric electron content variations before earthquakes in Southern California, 2003–2004, *J. Geophys. Res.*, 112, B02106, doi:10.1029/2006JB004447.

Dobrovolsky, I. P., S. I. Zubkov, and V. I. Miachkin (1979), Estimation of the size of earthquake preparation zones, *Pure Appl. Geophys.*, 117, 1025–1044, doi:10.1007/BF00876083.

Hao, Y. Q., Z. Xiao, and D. H. Zhang (2012), Multi-instrument observation on co-seismic ionospheric effects after great Tohoku earthquake, *J. Geophys. Res.*, 117, A02305, doi:10.1029/2011JA017036.

Heki, K., and Y. Enomoto (2013), Preseismic ionospheric electron enhancements revisited, *J. Geophys. Res. Space Physics*, 118, 6618–6626, doi:10.1002/jgra.50578.

Heki, K., and Y. Enomoto (2015), Mw dependence of the preseismic ionospheric electron enhancements, *J. Geophys. Res. Space Physics*, 120, 7006–7020, doi:10.1002/2015JA021353.

Kamogawa, M., and Y. Kakinami (2013), Is an ionospheric electron enhancement preceding the 2011 Tohoku-Oki earthquake a precursor?, *J. Geophys. Res. Space Physics*, 118, 1751–1754, doi:10.1002/jgra.50118.

Komjathy, A., L. Sparks, B. Wilson, and A. J. Mannucci (2005), Automated daily processing of more than 1000 ground-based GPS receivers to study intense ionospheric storms, *Radio Sci.*, 40, RS6006, doi:10.1029/2005RS003279.

Le, H., J. Y. Liu, and L. Liu (2011), A statistical analysis of ionospheric anomalies before 736 M6.0+ earthquakes during 2002–2010, *J. Geophys. Res.*, 116, A02303, doi:10.1029/2010JA015781.

Li, M., and M. Parrot (2013), Statistical analysis of an ionospheric parameter as a base for earthquake prediction, *J. Geophys. Res. Space Physics*, 118, 3731–3739, doi:10.1002/jgra.50313.

Masci, F. (2012), The study of ionospheric anomalies in Japan area during 1998–2010 by Kon et al.: An inaccurate claim of earthquake-related signatures?, *J. Asian Earth Sci.*, 57, 1–5, doi:10.1016/j.jseaes.2012.06.009.

Masci, F. (2013), Further comments on the ionospheric precursor of the 1999 Hector Mine earthquake, *Nat. Hazards Earth Syst. Sci.*, 13, 193–196, doi:10.5194/nhess-13-193-2013.

Masci, F., and J. N. Thomas (2014), Comment on "Temporal and spatial precursors in ionospheric total electron content of the 16 October 1999 M_w7.1 Hector Mine earthquake," by Su et al. (2013), *J. Geophys. Res. Space Physics*, 119, 6994–6997, doi:10.1002/2014JA019896.

Masci, F., J. N. Thomas, F. Villani, J. A. Secan, and N. Rivera (2015), On the onset of ionospheric precursors 40 minutes before strong earthquakes, submitted to, *J. Geophys. Res. Space Physics*, 120, 1383–1393, doi:10.1002/2014JA020822.

Michael, A. J. (2011), Random variability explains apparent global clustering of large earthquakes, *Geophys. Res. Lett.*, 38, L21301, doi:10.1029/2011GL049443.

Occhipinti, G., L. Rolland, P. Lognonné, and S. Watada (2013), From Sumatra 2004 to Tohoku-Oki 2011: The systematic GPS detection of the ionospheric signature induced by tsunamigenic earthquakes, *J. Geophys. Res. Space Physics*, 118, 3626–3636, doi:10.1002/jgra.50322.

Rolland, L., P. Lognonné, E. Astafyeva, A. Kherani, N. Kobayashi, M. Mann, and H. Munekane (2011), The resonant response of the ionosphere imaged after the 2011 Tohoku-Oki earthquake, *Earth Planet. Space*, 63, 853–857, doi:10.5047/eps.2011.06.020.

Thomas, J. N., J. J. Love, A. Komjathy, O. P. Verkhoglyadova, M. Butala, and N. Rivera (2012), On the reported ionospheric precursor of the 1999 Hector Mine, California earthquake, *Geophys. Res. Lett.*, 39, L06302, doi:10.1029/2012GL051022.

Xu, G., P. Han, Q. Huang, K. Hattori, F. Febriani, and H. Yamaguchi (2013), Anomalous behaviors of geomagnetic diurnal variations prior to the 2011 off the Pacific coast of Tohoku earthquake (Mw9.0), *J. Asian Earth Sci.*, 77, 59–65, doi:10.1016/j.jseaes.2013.08.011.